IChemE

0263–8762/01/$10.00+0.00

Trans IChemE, Vol. 79, Part A, March 2001

PROCESS VISCOSITY IN REVERSE ROLL COATING

S. ALONSO[1], O. RÉGLAT[2], F. BERTRAND[4], L. CHOPLIN[3] and P. A. TANGUY[4]

[1]*CIATEC, A.C. Omega 201, Leon, Gto, Mexico*
[2]*Coesi, Inc, Montreal, Canada*
[3]*GEMICO, ENSIC-INPL, Nancy, France*
[4]*Department of Chemical Engineering, École Polytechnique, Montreal, Canada*

The rheological behaviour of paper coating colours is investigated in the metering section of a laboratory reverse roll coater. The objective is to combine measurements of pressure in the metering nip, and torque on the metering rod to calculate the process viscosity. Classical rheological tests and nip flow numerical simulations are also required to complete the process viscosity evaluation. This viscosity is compared with that measured from step growth experiments in a rheometer. The process viscosity was found to be 2.5 to 6.3 times lower than the transient viscosity, depending on the coating colour formulation. The discrepancy observed between these two viscosities is mainly attributed to the rheological properties of the coating fluids. Furthermore, structure breakdown at relatively low shear rates suggests that steady state may not be reached in the metering nip. From numerical simulations, the pressure-driven contribution to the flow in the centre of the metering nip has been found constant in the case of Newtonian fluids, dependant on the shear-thinning index in the case of non-Newtonian fluids, and independent of inertia effects.

Keywords: metering nip; lubrication theory; process viscosity; transient viscosity; coating colour.

INTRODUCTION

Reverse roll coating is a technique commonly used in the coating industry to meter a thin fluid film on a moving substrate. During the film formation, the fluid is subjected to very high shear and extensional rates over a very short period of time. The fluid domain changes as a function of the hydrodynamic pressure within the nip as a result of the deformable cover usually used on one of the rolls. The free surface also adds more complexity to the flow due to the force equilibrium in the fluid-gas interface. Last of all, the rheological behaviour of the coating fluid is usually non-Newtonian, so the metering flow hydrodynamics is finally very difficult to describe.

For many years now, researchers have used the lubrication theory as well as the full Navier-Stokes equations (CFD models) to investigate reverse roll coating flows (Greener and Middleman[1], Kang and Liu[2], Coyle[3–5], Fourcade *et al.*[6], Poranen and Niemisto[7]). For the lubrication theory, the main hypothesis is that inertia effects are neglected. When applied to reverse roll coating flows, it also assumes that the flow between the rolls is nearly parallel, so that $P = P(x)$, $V_x \gg V_y$, and $\partial/\partial x \ll \partial/\partial y$, where P is the pressure and V_x the velocity in the main flow direction. Under these assumptions, the lubrication flow can be represented by[1]

$$\frac{\mathrm{d}P}{\mathrm{d}x} = \mu \frac{\partial^2 v_x}{\partial y^2} \tag{1}$$

The main difficulty in solving equation (1) is that of the specification of correct inlet and outlet boundary conditions. Greener and Middleman[1], using both vanishing pressure and pressure gradient as boundary conditions, predicted the coating thickness on the transfer roll for a relatively narrow range of metering rod to transfer roll speed ratios, although the flow rate deviated from the predictions of the model due to some recirculations upstream from the nip. However, investigations of the complete metering flow indicated that lubrication theory should be accurate in that region (Benkreira *et al.*[8], Coyle *et al.*[3,4]). Coyle *et al.*[3] showed that the metered nip flow deviates from the lubrication theory predictions at high speed ratios and capillary numbers. The dynamic wetting line moves towards the nip centre, the nip length shrinks, and the film thickness passes through a minimum. In another investigation, Coyle *et al.*[4] numerically showed, for a half-flooded nip, the existence of secondary flow downstream from the nip. This recirculation becomes smaller and finally disappears when the speed ratio is gradually increased, which has also been experimentally shown by Gaskell *et al.*[9]. Coyle *et al.*[4] found that the lubrication theory can be safely applied for speed ratios lower than about 0.5, and when gravity effects can be neglected. They also showed that the recirculations that apparently made the results of Greener and Middleman[1] deviate were not determinant in the flow rate calculations. The recirculations were always located in the same region, so that if the speed ratio was decreased, the free surface rose to accommodate the recirculations beneath it.

Kang and Lieu[2], following experimental observations, reported that the speed ratio below which inertia effects can be neglected is a function of the capillary number, namely

$$S_R = 0.29 Ca^{-0.54} \tag{2}$$

where S_R is the speed ratio of the metering rod to the applicator roll and Ca the capillary number ($V_t\mu/\sigma_T$) which measures the ratio of viscous forces to surface tension

forces. According to the authors, equation (2) is valid for a Reynolds number ($pV_t h/\mu$) between 0.3 and 30.4.

The influence of the rheological behaviour of the coating fluids on the flow hydrodynamics has also been investigated in reverse roll coating flows; the final conclusions reasonably agree. Greener and Middleman[1] showed that the behaviour of elastic liquids fits well with the Newtonian theory at low shear rates (100 to 1000 s^{-1}). Benkreira *et al.*[8] reported that the behaviour of purely shear-thinning fluids should be slightly different from that observed with Newtonian fluids. Coyle *et al.*[5], when working with elastic and inelastic shear-thinning fluids, showed that, from theoretical and experimental standpoints, the non-Newtonian rheological behaviour of a liquid should have little effect on the flow hydrodynamics. For highly elastic fluids, however, the flow can be strongly affected. In particular, they noted that elasticity decreases the film thickness, and the ribbing instability becomes irregular and time dependent. Furthermore, a small amount of polymer additives in the fluid can increase the wipe ratio and stabilize the flow if a long-chained polymer molecule is used (Kang *et al.*[10]). Finally, particle suspensions and Newtonian fluids behave differently at high speed in terms of the instabilities that are generated. For particle suspensions, the ribbing is smaller and more sensitive to the operating conditions (Réglat and Tanguy[11]).

Reverse roll coating flows find important applications in the paper coating industry; specifically, the metering operation on a film transfer coater (Metering Size Press) is nothing but a high speed reverse roll coating process. Most publications on the hydrodynamics in reverse roll coating flows have focused on low speeds and one-phase liquids. On the contrary, paper coating processes require the application of highly concentrated suspensions, that is, fluids which exhibit a complex rheological behaviour: shear-thinning is commonly observed at low shear rates; at high shear rates (above 1000 s^{-1}), the colour may be either Newtonian or shear-thickening, depending on the formulation (Laun and Hirsch[12]), Roper and Attal[13], Réglat and Tanguy[11], Alonso *et al.*[14] 2000a) and finally, elasticity is usually seen at low deformation (Laun and Hirsch[12]).

In the reverse flow conditions of the metering nip of a MSP, the film formation obeys a series of steps that makes the history of deformation very complex: the liquid is subjected to a moderate level of deformation rate during the preparation process; then, to a sudden increase of shear rate as it passes through the nip, and finally to very low shear rates during leveling (Figure 1). In classical rheometry, the closest tests to simulate the film formation mechanisms are the step growth and step relaxation experiments. These have already been used to investigate the

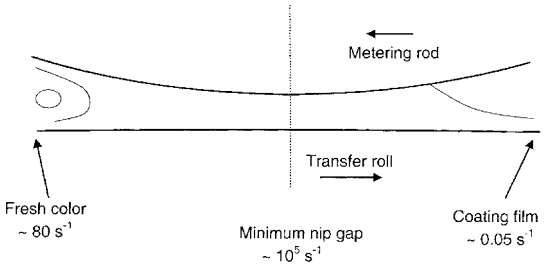

Figure 1. Typical shear rates in the metering nip.

colour behaviour in coating processes. Laun and Hirsch[12], when studying industrial coating formulations at different solids contents (62% to 70%), found that such experiments led to an overshoot in viscosity that increased with solids content. Nevertheless, at a shear rate of 4000 s^{-1} and solids contents lower than 62%, the coating colours hardly exhibited any overshoot. Cohu and Magnin[15], when carrying out step growth experiments with paints, observed overshoots in shear stress that diminished when increasing the imposed shear rate; at a shear rate of 7500 s^{-1}, no overshoot was observed. They concluded that in the roll coating process, where the shear rates are much higher, one should not expect viscosity overshoots. Yziquel *et al.*[16] found response overshoots when performing start-up tests with coating colours containing PVA. An overshoot in the transient viscosity was observed; it increased when the value of the initial shear rate of the experiment was increased. The same tests were performed with coating colours containing CMC, but the overshoot behaviour was reversed, i.e., the overshoot decreased when increasing the shear rate.

The rheological behaviour of paper coating colours can be investigated *in situ* by using the coater itself as a viscometer. By doing so, all the factors contributing to the behaviour of the suspension can be better accounted for: shearing history, field of deformation, and speed. Vidal *et al.*[17] were to the authors' knowledge the first to determine the coating colour viscosity directly in a blade coater. They evaluated the shear stress as function of the blade deformation, and the shear rate as function of the coating thickness. They found that the colours exhibited shear-thinning behaviour in the process, but a viscosity slightly different from that in a capillary rheometer. Réglat and Tanguy[11], in reverse roll coating, investigated the rheological behaviour of $CaCO_3$ suspensions and compared the process viscosity within the nip with that in a rheometer. By means of a pressure transducer fitted to the surface of the metering rod, they measured the pressure profile within the metering nip. By using different Newtonian fluids, the maximum pressure was employed to build a master curve, which they used to evaluate the viscosity of suspensions. They found that the process viscosity was much higher than that determined in a classical rheometer at steady state (Couette geometry), which may be due to the shear-thickening behaviour at high shear rates usually developed by aqueous suspensions (Thibault[18]). Alonso *et al.*[14] proposed a new procedure to obtain a coating colour process viscosity from torque measurements, although a calibration curve with Newtonian fluids was required. They compared it with that based on pressure measurements[11]. Although both procedures gave different results, they confirmed the irrelevance of the viscosity values obtained from classical rheometry to describe the colour rheological behaviour in the nip gap between rolls. These results are in agreement with what had been suggested earlier by Kistler and Scriven[19]: fluids behave differently in conventional rheometers and within coating nips.

This paper is a further contribution to the evaluation of process viscosity in paper coaters. The objective is to propose a novel method that combines both torque and pressure, steady state rheological measurements and numerical simulations to evaluate the coating colour process viscosity. The method is based on the lubrication theory, which is applied in the nip centre region with no calibration curve

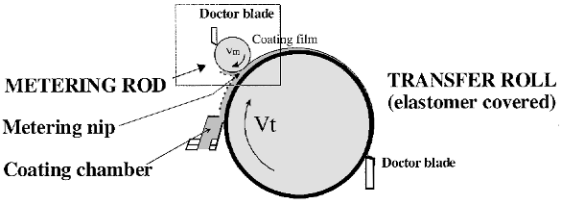

Figure 2. Laboratory reverse roll coater.

required as with former methods. The process viscosity is compared with that measured in transient conditions in a rheometer, a more realistic method to study the hydrodynamics of the metering nip.

EXPERIMENTAL

A laboratory reverse roll coater is used for the measurements (Figure 2). A full description of this apparatus is given by Réglat and Tanguy[20] and Alonso *et al.*[14] The metering rod of this coater (Figure 3) is fully instrumented with a wall-mounted piezoelectric transducer (response frequency of 250 kHz) to obtain the nip pressure profile. A torquemeter is directly connected to the shaft of the metering rod. Two displacement transducers, both located at the rod extremities, measure the position of the metering rod with respect to the undeformed surface of the transfer roll.

Several coating formulations (100 parts of clay used as dry basis) were considered in this work (Table 1). To prepare the suspensions, the dispersant was first added to the amount of deionized water necessary to achieve the target solids percentage. The slurries were made by slowly adding the clay with a volumetric feeder. Then, the latex suspension was added, followed by (previously hydrated) carboxymethyl cellulose (CMC), under continuous agitation. The colours were mixed for a minimum of 30 minutes before the pH was adjusted to 8.0 by adding NaOH. At the end, the coating colours were mixed for an additional 60 minutes to stabilize the suspension.

PROCESS VISCOSITY THEORETICAL BASIS

The theoretical development is based on the lubrication theory applied in the nip core region (Figure 4). It is delimited by the two dotted vertical lines between which the pressure gradient is essentially constant, as shown in Réglat and Tanguy[11,20]. In this section, inertia forces are negligible and the streamlines are almost parallel[1,3,4]. In addition to the above realistic assumptions, it is further supposed that the deformation of the transfer roll is such that the nip gap is almost constant (Carvalho and Scriven[21], Fourcade *et al.*[6]).

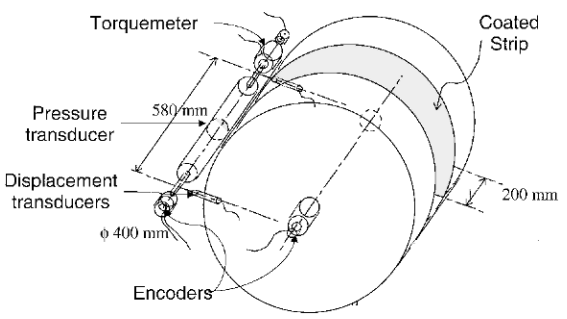

Figure 3. Instrumentation of the metering section of the mini coater.

Table 1. Coating colour formulations (pph of clay basis).

LABEL	Clay	Dispersant	Latex	CMC	% Solids
A	100	0.04	10	0.25	61.0
B	100	0.04	10	0.50	61.0
C	100	0.04	10	1.00	61.0
D	100	0.04	10	0.50	56.0
E	100	0.04	10	0.50	63.3

Since both torque and pressure measurements take place on the surface of the metering rod, the lubrication theory (equation (1)) is applied on the rod. There, the shear rate is approximated as

$$\left.\frac{\partial v_x}{\partial y}\right|_{wall} \equiv \frac{V_t}{h}\alpha \tag{3}$$

where V_t is the transfer roll speed and h the nip gap.

Equation (1) implies that the velocity profile is parabolic, with a combination of Couette and Poiseuille flows[15,21]. The parameter α is defined as the contribution of the Poiseuille flow on the resulting Couette velocity gradient evaluated at the wall, namely

$$\alpha = \left.\frac{\left.\frac{\mathrm{d}v_x}{\mathrm{d}y}\right|_{Couette+Poiseuille}}{\left.\frac{\mathrm{d}v_x}{\mathrm{d}y}\right|_{Couette}}\right|_{wall} \tag{4}$$

Using equation (1) and equation (4), the process viscosity can be expressed as (see Appendix)

$$\mu_{proc} = \frac{T^2}{V_t \frac{\mathrm{d}P}{\mathrm{d}x}(SR)^2\,\alpha} \tag{5}$$

The procedure by which equation (5) was obtained does not require a Newtonian fluid to be used as a reference as in previous studies[11,14]. The evaluation of the process viscosity can be made directly from torque and pressure measurements combined with the rheological characterization of the fluid at steady state and numerical simulations of the metering nip flow.

Numerical simulations are needed to evaluate the parameter α, since it is not accessible experimentally.

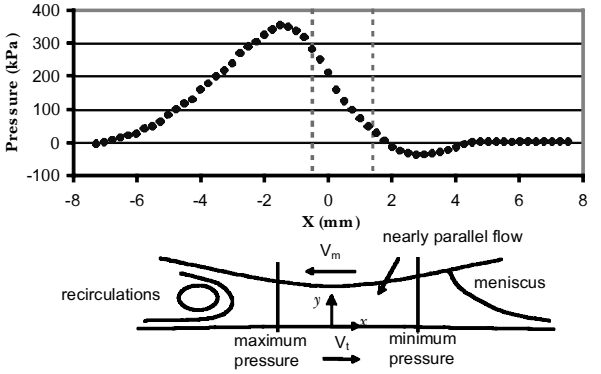

Figure 4. Characteristic pressure profile in the metering nip.

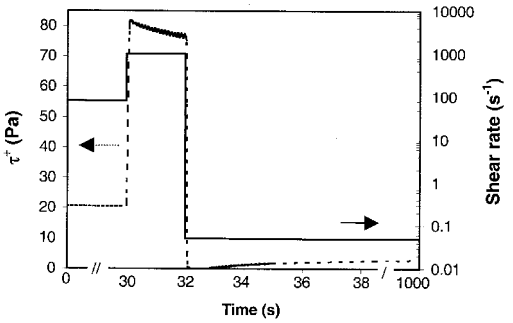

Figure 5. Transient shear stress response of the coating colours.

Commercially available CFD software POLY2D™ was used for this purpose. The nip is fully flooded, deformable, and the metering rod speed is 0.5 m s^{-1} rotating in reverse mode. The two-dimensional Navier-Stokes equations were solved with the finite element method. It should be mentioned that POLY2D™ was adapted to solve the deformation of the transfer roll (see details in Fourcade *et al.*[6]). About 4000 quadratic triangular elements with six nodes in velocity and one in pressure were used in each simulation for the fluid domain. The solid domain required about 5000 elements. Each simulation was carried out by first solving the fluid problem and considering that the coating colours obey the Cross model. The pressure and stresses fields were then calculated and used to deform the transfer roll surface. As a result, a new fluid domain was created and remeshed, and the fluid problem was solved again. This iterative procedure was used until convergence of the solid-fluid interface[6]. At the very beginning, the mesh was tested and refined so that the results were not dependent on the mesh size. In the centre, a layer of 5 elements was required to obtain accurate calculations of the Poiseuille contribution α.

RESULTS AND DISCUSSION

Metering Nip Flow Simulation in the Rheometer

To investigate the coating colours, rheological behaviour through the nip, stress growth tests were carried out to mimic the metering nip flow conditions. A Rheometrics RFX II rheometer was used for that purpose. The tests started (continuous line) with an initial pre-shear of 80 s^{-1} during 30 s, a typical value induced by the flow in the coating make-down step[11]. It was followed by a abrupt rate increase to 1000 s^{-1} (stress growth), which was maintained during two seconds. Although far from what actually occurs in the nip, these two values in shear rate and time were the best compromise that could be obtained with the rheometer to describe the nip hydrodynamics. At the end, the shear rate was brought down to 0.05 s^{-1} (stress relaxation) to simulate the rate of leveling of the film on the transfer roll (Macosko[22]).

The transient stress τ^+ response (dotted line) of the coating colours is shown in Figure 5. At the end of the pre-shearing stage, the steady state is already reached. The sudden stress growth results in a small overshoot in shear stress, which is attributed to shear-induced rearrangements of the coating structure in the gap[12]. After the two second lapse, the stress relaxation produces a rapid decrease of the transient shear stress because of the reduction in the shear rate; however, τ^+ increases slowly with time, and so does the transient viscosity η^+ due to the structure build-up of the coating colour at very low shear rates. In this work, it was observed that the overshoots increased with shear rate, CMC concentration, and solids content. The overshoots were found at short times, as expected[22], but the response times were significantly larger than those occurring in the metering nip, which suggests that steady state may not be reached in the metering nip. The overshoots were observed with all formulations, similarly to what has been observed with other coating colour formulations[12,16].

Following the same procedure as in Figure 5, tests were performed on all coating colours, but with different stress growth levels (the shear rates varied between 100 s^{-1} and 1500 s^{-1}). The results in Figure 6 (for coating formulation C) show that the higher the shear rate imposed in the stress growth step, the lower the transient viscosity after the two seconds of shearing, which is explained by the shear-thinning behaviour of the samples, and the lower the eventual value of η^+ (measured 1000 s after the stress relaxation step). The recovery time seems to be proportional to the stress growth level and appears to be very large. Consequently, the Deborah number (the ratio of the fluid relaxation time to the characteristic process time) is also expected to be large, so that elastic stresses are expected to dominate.

The coating process can also be analysed in terms of deformation (the product of shear rate and time). From a theoretical standpoint, there is a critical deformation above which the internal structure in the fluid is completely destroyed so that steady state is reached. The smallest deformation (evaluated after the 2 seconds of the step growth experiment) shown in Figure 6 is about the same order of magnitude as that expected in the process, a deformation level at which coating colour breakdown may have already started. At higher deformations, the coating colour takes more time to recover. Complete structure breakdown is not reached at very large deformations and the process viscosity becomes a relevant parameter in the process. Therefore, the viscosity of the coating colours arriving in the application nip is very likely lower than that shown in Figure 6, since the shearing in the metering nip is very significant ($\sim 10^5$ s^{-1}), and the time the coating colour film has to relax under a shear rate of about 0.05 s^{-1}, from the metering nip to the application nip, is substantially lower ($\sim$0.04 s at 1250 m min^{-1}); in fact, it may be very close to its viscosity just after leaving the metering nip.

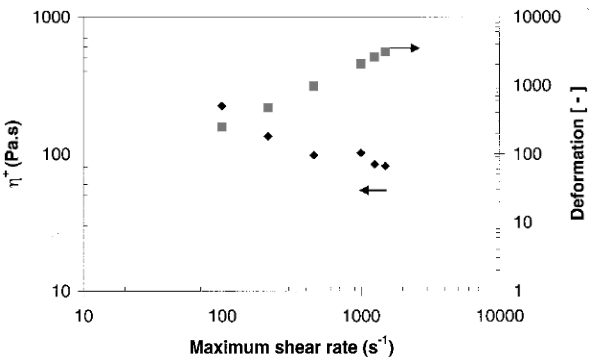

Figure 6. Rheological behaviour of coating colour C.

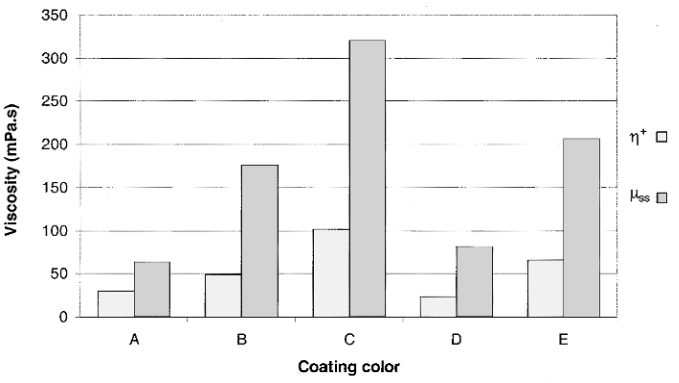

Figure 7. Comparison of eventual transient viscosity with steady state viscosity.

In Figure 7, the transient viscosity η^+ measured after the stress relaxation step is compared with the steady state values μ_{ss} at low shear rate ($0.05\,s^{-1}$) obtained without pre-deformation of the samples. The viscosity of the coating colours, those which were subjected to the shearing history, is consistently lower. Indeed, some structure breakdown occurred during the tests[12,15].

Steady State and Oscillatory Tests

To further characterize the coating colours, steady state shear rate measurements and small amplitude oscillatory shear tests within the linear viscoelastic region were also performed. All coating colours are shear-thinning at low shear rates (Figure 8), and for all of them, the viscosity levels off at high shear rates[16]. The power law fits fairly well with a viscosity plateau at very high shear rates (Table 2), where the coating colours behave as Newtonian. Furthermore, as shown in Figure 9, the storage modulus G' increases with the CMC concentration, solids contents, and frequency, and it is one order of magnitude larger than the loss modulus G'' (not shown). Such a response is typical of a solid-like behaviour, where the strong particle-particle interactions, the break-up and build-up of structures, and the particle alignment govern the coating colour behaviour (Carreau and Lavoie[23]). The corresponding phase angle was found always lower than 15°, confirming the elastic behaviour of the formulations at very small deformation.

Nip Process Viscosity Evaluation

In order to evaluate the process viscosity, the laboratory coater was operated with the following parameters:

- Transfer roll speed: $1250\,m\,min^{-1}$.
- Metering rod speed: $30\,m\,min^{-1}$.
- Load per unit width: $1\,kN\,m^{-1}$.

Table 2. Parameters of coating colours following the model $\mu_{pl} = m\gamma^{n-1} + \eta_\infty$.

Coating colour Label	m (Pa s^n)	n	η_∞ (Pa s)	$\lvert(\mu_{ss} - \mu_{pl})/\mu_{pl}\rvert$
A	5.0	0.220	0.044	0.056
B	10.5	0.170	0.063	0.072
C	16.0	0.145	0.090	0.081
D	3.70	0.220	0.027	0.058
E	11.5	0.184	0.088	0.073

These conditions correspond to an operating range where good runnability was obtained (no spitting, no air entrapment). They are also fully compatible with current industrial paper coating operating conditions (Pauksta[24]). Furthermore, the minimum critical speed ratio calculated from equation (2) lies just above the speed ratio used in this work ($V_m/V_t = 0.024$), but all these cases correspond to Reynolds numbers[2] in the range [9.04–27.13], below the upper limit of 30.4. Strictly speaking, in terms of the speed ratio (from equation (2)), lubrication theory cannot be applied to this problem; however, that lower limit arose because it was the lower speed ratio for which the experimental apparatus was designed, not from limitations in the applicability of the lubrication theory[2]. Therefore, it is assumed that equation (2) still applies to the problem.

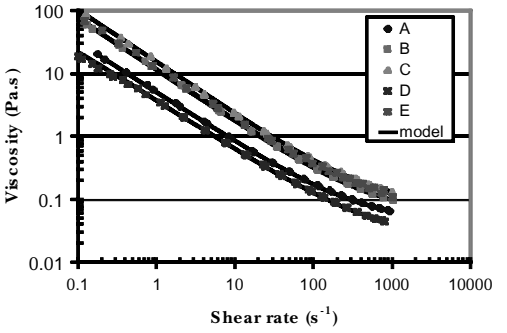

Figure 8. Shear viscosity of the coating colours at different CMC concentrations.

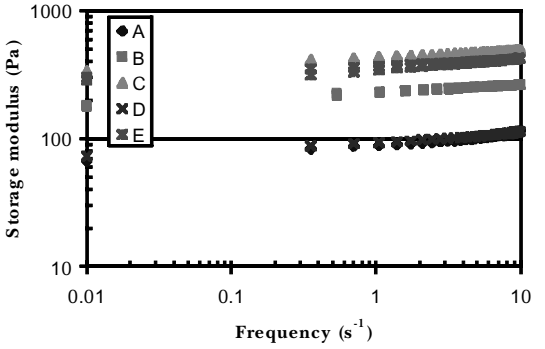

Figure 9. Storage modulus of the coating colours.

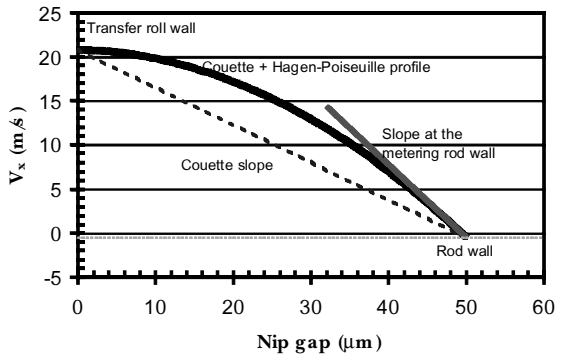

Figure 10. Numerical velocity profile in the centre of the metering nip ($V_t = 1250\,\mathrm{m\,min^{-1}}$, $\mu = 75\,\mathrm{mPa,s}$, $V_m = 0.5\,\mathrm{m\,s^{-1}}$, nip gap$= 50\,\mu\mathrm{m}$).

The physical meaning of the pressure-driven contribution α is now discussed. Equation (5) implies that all the measurements are to be made on the wall of the metering rod, where both torque and pressure are actually measured. The dotted line in Figure 10 represents the Couette contribution to the global flow. The parameter α, the Poiseuille contribution, added to the Couette flow gives the parabolic profile shown. Since the Poiseuille contribution to the flow is not accessible experimentally, numerical simulations were carried out at different nip gaps, Newtonian viscosities, and transfer roll speeds. Table 3 shows the values for the different operating conditions; α at the wall is practically constant in all cases and independent of viscosity for the conditions considered in this work. Therefore, in the region of nearly constant pressure gradient, the flow is equivalent to a Couette flow with a constant pressure-driven contribution[21], independent of the Newtonian viscosity, nip gap and speed.

For the coating colours, the same numerical procedure was carried out with the Cross model since the power law model leads to infinite viscosities at low shear rates, a fact that cause computational problems[13]. The plateau in viscosity at low shear rates makes the Cross model computationally efficient and simple to fit the experimental data for the simulation purposes. However, the Cross model can only describe pure shear-thinning fluids, so that the elasticity of the coating colours was not considered in the simulations. The low shear-rate viscosity plateau η_o was imposed at 500 Pa s, since lower values did not affect significantly the global hydrodynamics of the flow. The Cross model rheological parameters for the coating colours are shown in Table 4. Those values were obtained by fitting the Cross model parameters to the steady state rheological curve obtained in the rheometer. The parameter α increases with respect to the shear-thinning index p as shown in Table 5, but then it reduces to nearly the Newtonian limiting value. At high values of p, the shear rates developed in the centre of the nip are such that the rheological behaviour of the coating colours is that of the Newtonian plateau at very high shear rates.

Table 4. Parameters of coating colours obeying the Cross model $\mu_{Cr} = \eta_\infty + [\eta_o - \eta_\infty]/[1 + (t\gamma)^p]$.

Coating colour Label	t (s)	p	η_o (Pa s)	η_∞ (Pa s)	$\lvert(\mu_{ss} - \mu_{Cr})/\mu_{Cr}\rvert$
A	290	0.80	500	0.044	0.062
B	87	0.84	500	0.063	0.083
C	62.5	0.83	500	0.082	0.095
D	1100	0.76	500	0.028	0.081
E	83	0.82	500	0.080	0.094

Another important result from the simulations was that the values of α shown in Tables 3 and 5 were independent of inertia forces. Certainly, inertia does affect the hydrodynamics of the flow upstream and downstream from the nip by changing the location and the shape of the recirculations, but in the centre of the nip, inertia effects are unimportant.

From the numerical simulations, another correction had to be made with respect to the torque. The torquemeter used in the experiments implicitly measures the integral of the stress forces exerted by the fluid on the rod surface. Equation (5) requires the torque, but only the integral of the stress forces over the region within which the pressure gradient is constant. A typical tangential force profile is shown in Figure 11 (the numerical model included in every case the rheological parameters of Table 4). Since the deformation of the roll and the nip gap are the result of an equilibrium of hydrodynamic forces (Réglat and Tanguy[11,14], Alonso *et al.*[25]), the pressure peak was used as a reference parameter to categorize the flow hydrodynamics. The experimental and calculated torques were compared when the calculated maximum pressure was equal to that measured in the experiments at the same operating conditions. The total torque applied on the rod corresponds to the integral of the curve in Figure 11, i.e., the summation of the positive and the negative areas. The total torques were first compared, and then the local torque in the region of interest was inferred (the small region around which the maximum is located). The measured torque in the experiments overpredicted by between 10% and 20% the tangential force in the region of almost constant pressure gradient, depending on the

Table 3. Numerically evaluated ratio of Poiseuille to Couette contributions to the flow in the centre of the metering nip for Newtonian fluids.

	Nip gap (μm)							
	25		50		75		100	
	Newtonian Viscosity (mPa s)							
α V_t (m min^{-1})	84	104	84	104	84	104	84	104
1000	1.93	1.94	1.94	1.95	1.95	1.93	1.92	1.93
1250	1.93	1.93	1.95	1.96	1.96	1.94	1.95	1.94
1500	1.93	1.94	1.95	1.96	1.96	1.95	1.96	1.95

Table 5. Numerically-evaluated ratio of Poiseuille to Couette contributions to the flow in the centre of the metering nip at different rheological parameters.

α	shear-thinning index p of the Cross model					
V_t (m min^{-1})	0.2	0.4	0.6	0.7	0.8	0.84
1000 ($t = 87$)	2.11	2.39	2.10	1.99	1.99	1.99
1500 ($t = 87$)	2.07	2.15	2.07	2.02	2.01	2.00
1250 ($t = 62.5$)	2.08	2.21	2.07	2.00	1.98	1.99
1500 ($t = 62.5$)	2.07	2.20	2.07	2.01	1.99	1.98

Table 6. Correction factors of the experimental torque measurements.

Coating colour Label	Correction
A	0.90
B	0.85
C	0.85
D	0.90
E	0.85

coating colour (Table 6). The experimental torque measurements were accordingly corrected.

To verify the validity of equation (5), Newtonian fluids were used. They consisted of polyethylene glycol solutions at three concentrations (w/w): 13.2%, 17%, and 18.3%, yielding viscosities of 43 mPa s, 84 mPa s, and 104 mPa s, respectively. The differences between the shear viscosity and the process viscosity evaluated from equation (5) are less than 11%. It is believed that the disagreement is due to experimental errors, the assumptions underlying the analytical development of equation (5), and the assumptions implicit in the numerical model when calculating the constant α and the torque corrections.

Figure 12 shows the results of the process viscosity μ_{proc} against the transient viscosity 0.1 s after the stress growth at 1000 s^{-1}, where the overshoot in shear stress is maximum (the interval of 0.1 s corresponds to the time it takes the rheometer to change the shear rate from 80 s^{-1} to 1000 s^{-1}; during this period the actual shear rate is unknown). Both transient and process viscosities increase almost linearly with the CMC concentration (the dotted line represents the case when the process viscosity equals η^+). Since all coating colours are below the dotted line in Figure 12 (left), it follows that the higher shear rates encountered in the process broke down the coating structure more rapidly than in the step growth experiments, with a shear-thinning degree higher than that deduced from rheological measurements. The proportional increase of both process and transient viscosities can be seen as the effect of the viscous behaviour of the coating colours. The separation from the dotted line may be explained by the increased shear-thinning behaviour in the nip.

Figure 12 (right) shows the influence of the solids content. When there are more particles, the values depart from the dotted line, a behaviour also encountered when increasing the thickener concentration (Figure 12, left). Within the metering nip, the amount of solids plays a dominant role in the behaviour of coating colour E by increasing its process viscosity. Although coating colours C and E have comparable rheological properties as inferred from classical rheological measurements, the increased shear rate in the nip may appreciably reduce the shear-thinning degree of coating colour E. As a result, the viscosity of coating colour E is higher in the metering nip than that predicted from classical rheology.

Elasticity may contribute to that separation between the process and transient viscosities if normal stresses are important. Since the overshoots increase with shear rate, but they occur at short times, very high changes in shear at very short times—very high deformation rates as those in the metering nip—may maintain the coating colours within the viscoelastic region, before reaching its steady state. Under those circumstances, the corresponding normal stresses would affect both torque and pressure. The torque is lower than 1 Nm, so that an increase in its value would actually decrease the process viscosity (see equation (5)). The same response would be seen if the total pressure within the nip were increased. Elastic stresses developed by the flow are believed to be unimportant[23] since the samples did not show any shear-thickening behaviour, which has been shown to induce normal stresses at very high shear rates[12].

It should be also kept in mind that the parameters used in metering flow simulation in the rheometer, tests from which the transient viscosity was obtained, are very different from what actually occurs in the nip. A better compromise from the performance of the rheometer may significantly change the measurements of the transient viscosity. Since the overshoots were found to increase with shear rate, CMC concentration, and solids content, either a decrease in the response time or and increase in the step shear rate would cause an ever higher transient

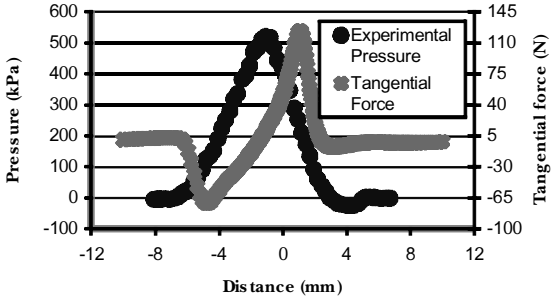

Figure 11. Calculated tangential force and its corresponding experimental pressure profile for coating colour D ($V_t = 1250$ m min^{-1}, $V_m = 30$ m min^{-1}, numerical nip gap = 35 μm).

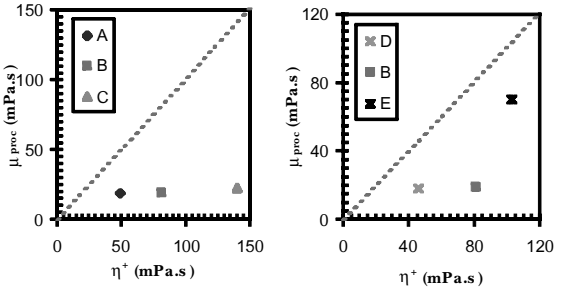

Figure 12. Process viscosity for the coating colours at different CMC concentrations (left) and solid contents (right).

viscosity, increasing the difference between both process and transient viscosities.

From the results, the process viscosity becomes relevant in understanding the metering nip flow. It is believed that the viscosity of the fluid arriving in the application nip is the process viscosity in the metering nip, since the relaxation time is about six orders of magnitude longer than the residence time on the transfer roll. As a result, the process viscosity may give new insights in understanding the runnability of the coating colours in the application nip. Runnability problems in the application nip may also be better understood. For example, by knowing the viscosity of the coating colours in the metering nip, it would be possible to predict the premetered film coating thickness (Grön *et al.*[26]); thus, the specific pressure on the application nip, according to the base paper properties, could be specified for a desired film transfer ratio[26].

CONCLUDING REMARKS

The objective was to investigate the rheological behaviour of coating colours in reverse roll coating. Rheological measurements were carried out to represent what actually occurs in the metering process. A laboratory coater was used and a new method was proposed to evaluate the coating colours viscosity in the metering nip. Two important parameters in reverse roll coating were used in the procedure: the pressure gradient and the metering rod torque signal; additionally, classical rheological measurements and numerical simulations were carried out. Lubrication theory was applied in a region where the pressure gradient is almost constant, relatively far from the location of the instabilities. The method proposed in this work made it possible to evaluate the process viscosity, which was found different from that obtained by transient tests in a classical rheometer. The process viscosity was 2.5 to 6.3 times lower than the transient viscosity, depending on the coating colour formulation. It was also shown that the structure breakdown of the coating colour may be such that steady state is not reached in the metering nip. Moreover, the viscosity of the coating colours arriving in the application nip is probably very close to that leaving the metering nip. Finally, numerical simulations showed that there is a constant pressure-driven contribution to the flow in the centre of the nip, where inertia effects do not play a significant role.

APPENDIX

The complete mathematical development presented here was carried out to evaluate the process viscosity. Neglecting inertia effects in the Navier-Stokes equations, the momentum balance for the lubrication flow is[1]

$$\frac{\partial^2 v_x}{\partial y^2} = \frac{1}{\mu}\frac{\partial P}{\partial x} \tag{A1}$$

Equation (A1) implies that the velocity profile is parabolic. It is in fact a combination of Couette and Hagen-Poiseuille flows[15,21]. By integrating equation (A1), then

$$\frac{\partial v_x}{\partial y} = \frac{1}{\mu}\frac{\partial P}{\partial x} y + C_1 \tag{A2}$$

If a small velocity gradient is assumed on the surface of the transfer roll ($y = 0$), then (see Figure 10)

$$C_1 \cong 0 \tag{A3}$$

and equation (A2) becomes

$$\frac{\partial v_x}{\partial y} = \frac{1}{\mu}\frac{\partial P}{\partial x} y \tag{A4}$$

If the small speed ratio used in reverse roll coating paper applications (metering size press) is considered, and if it is assumed that the roll curvature is very small near the region of nearly constant pressure gradient, the shear rate on the wall of the metering rod can be approximated by

$$\left.\frac{\partial v_x}{\partial y}\right|_{wall} \cong \frac{V_t}{h}\alpha \tag{A5}$$

where V_t is the transfer roll speed, h the nip gap, and α represents the contribution of the Hagen-Poiseuille flow on the resulting velocity gradient evaluated at the wall near the centre of the nip. By combining equation (A4) and equation (A5) then

$$\alpha\frac{V_t}{h} = \frac{1}{\mu}\frac{\partial P}{\partial x} h \tag{A6}$$

Solving for μ in equation (A6)

$$\mu = \frac{1}{\partial V_t}\frac{\mathrm{d}P}{\mathrm{d}x} h^2 \tag{A7}$$

Now the relation between equation (A7) which expresses the dependence of the viscosity on the nip flow conditions, and the torque exerted by the metering rod on the fluid is established. From the Newton's law of viscosity

$$\left.\sigma\right|_{wall} = \mu\left.\frac{\partial v_x}{\partial y}\right|_{wall} \cong \mu\frac{V_t}{h}\alpha \tag{A8}$$

where $\sigma|_{wall}$ is the shear stress on the rod. This shear stress is related to the measured torque T exerted by the rod

$$\sigma|_{wall} = \frac{T}{SR} \tag{A9}$$

In this equation, S is the wetted area on the metering rod surface and R its radius. Solving for h in equation (A8) and substituting into equation (A7) yields

$$\mu = \frac{1}{\alpha V_t}\frac{\mathrm{d}P}{\mathrm{d}x}\left(\frac{\mu V_t}{\sigma|_{wall}}\right)^2 \tag{A10}$$

By using equation (A9), μ becomes the process viscosity that can be expressed as (equation (5) in the text)

$$\mu_{proc} = \frac{T^2}{V_t\frac{\mathrm{d}P}{\mathrm{d}x}(SR)^2\alpha} \tag{A11}$$

where α depends on the rheological behaviour of the fluid and can be estimated numerically.

NOMENCLATURE

h	nip gap in the lubrication region
m	consistency index in the Power law rheological model
n	shear-thinning index in the Power law rheological model
$\mathrm{d}P/\mathrm{d}x$	pressure gradient in the lubrication region
p	shear-thinning index in the Cross rheological model
R	radius of the metering rod
S	wetted surface of the metering rod

S_R ratio of metering rod speed to transfer roll speed
t consistency index in the Cross rheological model
T effective torque measured on the metering rod
V_x velocity in the main flow direction
V_y velocity in the transverse flow direction
V_t transfer roll speed
x main flow direction
y transverse flow direction

Greek symbols
α Poiseuille contribution to the flow in the centre of the nip
η_o viscosity plateau at low shear rates for the Cross model
η_∞ viscosity plateau at very high shear rates
η^+ transient viscosity from the rheometer
μ shear viscosity
μ_{Cr} viscosity calculated from the Cross rheological model
μ_{pl} viscosity calculated from the power law rheological model
μ_{ss} shear viscosity from the rheometer at steady state
μ_{proc} process viscosity
σ_T surface tension
σ characteristic shear stress in the centre of the metering nip

REFERENCES

1. Greener, J. and Middleman, S., 1981, Reverse roll coating of purely viscous liquids, *Ind Eng Chem Fundam*, 20 (1): 63–66.
2. Kang, Y. T. and Liu, T. J., 1991, Minimum film thickness for reverse roll coating, *Chem Eng Sci Short Comm*, 46 (11): 2958–2960.
3. Coyle, D. J., Macosko, C. W. and Scriven, L. E., 1990, The fluid dynamics of reverse roll coating, *AIChE J*, 36 (2): 161–174.
4. Coyle, D. J., Macosko, C. W. and Scriven, L. E., 1990, A simple model of reverse roll coating, *Ind Eng Chem Res*, 29 (7): 1416–1419.
5. Coyle, D. J., Macosko, C. W. and Scriven, L. E., 1990, Reverse roll coating of non-Newtonian liquids, *J Rheol*, 34 (5): 615–637.
6. Fourcade, E., Bertrand, F., Réglat, O. and Tanguy, P. A., 1999, Finite element analysis of fluid-solid interaction in the metering nip of a metering size press, *Comp Meth in Appl Mech and Eng*, 174: 235–245.
7. Poranen, J. and Niemistö, A., 1999, Experimental and theoretical study for metering size press, *Tappi Advanced Coating Fundamental Symp Proc, Toronto*, 159–161.
8. Berkreira, H., Edwards, M. F. and Wilkinson, W. L., 1981, Roll coating of purely viscous liquids, *Chem Eng Sci*, 36 (2): 429–434.
9. Gaskell, P. H., Innes, G. E. and Savage, M. D., 1998, An experimental investigation of meniscus roll coating, *J Fluid Mech*, 355: 17–44.
10. Kang, Y. T., Lee, K. Y. and Liu, T. J., 1991, The effect of polymer additives on the performance of a two-roll coater, *J Appl Polymer Sci*, 43: 1187–1195.
11. Réglat, O. and Tanguy, P. A., 1998, Rheological investigations of $CaCO_3$ slurries in the metering nip of a metering size press, *Tappi J*, 81 (5): 195–205.
12. Laun, H. M. and Hirsch, G. X., 1989, New laboratory tests to measure rheological properties of paper coatings in transient and steady-state flows, *Rheologica Acta*, 28 (4): 267–280.
13. Roper III, J. A. and Attal, J. F., 1993, Evaluations of coating high-speed runnability using pilot coater data, rheological measurements, and computer modeling, *Tappi J*, 76 (5): 55–61.
14. Alonso, S., Réglat, O., Bertrand, F. and Tanguy, P. A., 2000, Process viscosity in a film coater, *Paperi ja Puu—Paper and Timber*, 82 (1): 34–40.
15. Cohu, O. and Magnin, A. J., 1995, Rheometry of paints with regard to roll coating, *J Rheology*, 34: 767–785.
16. Yziquel, F., Moan, M., Carreau, P. J. and Tanguy, P. A., 1999, Non linear behavior of paper coating colors, *Nordic Pulp and Paper Research J*, 14 (1): 37–48.
17. Vidal, F., Egurreguy, D. and Pouyet, J., 1991, Rhéologie *in situ* des sauces de couchage, *Les Cahiers de Rhéologie*, IX (4): 171–179.
18. Thibault, F., 1999, Analyse du procédé de mélange solide-liquide: application à la préparation des sauces du couchage, *PhD Thesis*, (École Polytechnique de Montréal, Canada).
19. Kistler, S. F. and Scriven, L. E., 1984, Coating flow theory by finite element and asymptotic analysis of the Navier-Stokes system, *Int J Num Meth in Fluid Mech*, 4: 207–229.
20. Réglat, O. and Tanguy, P. A., 1997, Experimental study of the flow in the metering nip of a metering size press, *AIChEJ*, 43 (11): 2911–2920.
21. Carvalho, M. S. and Scriven, L. E., 1997, Deformable roll coating flows: steady state and linear perturbation analysis, *J Fluid Mech*, 339: 143–172.
22. Macosko, C. W., 1994, *Rheology, Principles, Measurements, and Applications*, (VCH Publishers, USA).
23. Carreau, P. J. and Lavoie, P. A., 1993, Rheology of coating colors: a rheologist point of view, *Proc of the Tappi Advanced Coating Fundamentals Symp, Minneapolis*, 1–12.
24. Pauksta, P. M., 1998, Speed: its effect on coating equipment and formulations, *Tappi J*, 81 (8): 58–60.
25. Alonso, S. and Tanguy, P. A., 2000, Hydrodynamic instabilities in the metering nip of a film coater, *Tappi J*, (Submitted).
26. Grön, J., Sunde, H. and Nikula, E., 1998, Runnability aspects in high speed film transfer coating, *Tappi J*, 81 (2): 157–165.

ACKNOWLEDGEMENTS

The financial contribution of Paprican and NSERC (Canada), and Conacyt (Mexico) are gratefully acknowledged. Also, the invaluable discussions with Mr Philippe Marchal (GEMICO ENSIC-INPL) about rheology and the use of the rheometer, and the helpful comments from Professor Pierre Carreau are sincerely appreciated.

ADDRESS

Correspondence concerning this paper should be addressed to Professor P. A. Tanguy, Department of Chemical Engineering, École Polytechnique, PO Box 6079, Station Centre Ville, Montreal, Canada H3C 3A7.

The manuscript was received 19 May 2000 and accepted for publication after revision 18 December 2000.